

Double-electron detachment cross sections in intermediate-energy H^- plus noble-gas collisions

J. S. Allen, X. D. Fang, A. Sen, R. Matulioniene, and T. J. Kvale
Department of Physics and Astronomy, University of Toledo, Toledo, Ohio 43606
 (Received 31 March 1994; revised manuscript received 30 March 1995)

Absolute measurements of the total double-electron detachment (DED) cross sections for 3- to 50-keV H^- ions incident on helium atoms and for 5- to 50-keV H^- ions incident on neon and argon atoms are reported in this paper. The present DED cross sections are in better agreement with the previously reported DED cross sections for helium targets than for either neon or argon targets. A semiempirical calculation of the double detachment cross sections for the intermediate-energy collision region is also presented in this paper.

PACS number(s): 34.70.+e

I. INTRODUCTION

Electron detachment is a significant reaction channel in intermediate-energy collisions between negative ions, which have low binding energies, and atoms. The H^- -noble-gas collision system is one of the most fundamental negative-ion-atom collision systems; therefore, experimental and theoretical studies of this collision system are useful for improving our understanding of the physics of negative-ion-atom interactions. Measurements of the cross sections for electron detachment in negative-ion-atom collisions are also of interest in fusion energy research, where negative-ion-atom collisions can be used to produce atomic beams for plasma heating, and in interpreting phenomena in various areas in astrophysics.

The literature contains the results from numerous experimental measurements [1-7] of double-electron detachment (DED) in collisions between 2- to 50-keV H^- ions and noble-gas atoms. Tawara and Russek [8] have reviewed the experiments reported before 1973, and McDaniel, Mitchell, and Rudd [9] have very recently reviewed the field for charge-changing collisions in the $H^{(-,0,+)}-He$ collisional systems. Even though the first measurements for double-electron detachment in this collisional system appeared in the literature over 30 years ago, we are not aware of any reported theoretical calculations for these systems in this collisional energy region. Furthermore, the discrepancies in the measured cross sections reported in the literature by the various experimental groups are still not fully resolved.

In this paper, we report absolute measurements of the total cross sections for double-electron detachment from the H^- ion in collisions between 3 to 50-keV H^- ions and helium atoms and 5 to 50-keV H^- ions and neon and argon atoms in order to address the discrepancies in the experimental data for double-electron detachment in H^- plus (He, Ne, and Ar) collisions and possibly to stimulate theoretical interest in this collision process. We also report the results of a semiempirical calculation of the double detachment cross sections for this collisional system. The results of this calculation are found to be in good agreement with the present experimental values of the

double detachment cross sections for helium targets but only in fair agreement for neon and argon targets.

II. EXPERIMENTAL METHOD AND ANALYSIS

A. Apparatus

The apparatus used to measure the double-electron detachment cross sections is described in Refs. [10] and [11]; therefore the apparatus is described only briefly below for continuity. The main components of this apparatus are (1) a relatively standard 3- to 50-keV negative-ion accelerator, including a duoplasmatron ion source system and acceleration column, which produces a fast negative hydrogen ion beam; (2) a beam drift and steering region; (3) a scattering chamber containing a noble-gas target cell; and (4) a charge-state analyzing magnet, which separates the H^- , H^+ , and H^0 ion and atom components of the beam exiting the noble-gas target cell, and three independent beam detectors, which simultaneously detect the three separated charge-state components of the scattered beam.

Negative hydrogen ions are extracted from a duoplasmatron ion source, focused by an einzel lens and mass-analyzed by a Wien filter to select only the H^- ion component of the beam. A calibrated, 0 to 50-keV power supply provides the accelerating voltage for the ions as they pass through the acceleration column, and then the fast H^- ions are collimated and directed into the noble-gas target cell. The H^- ions travel a distance of 3.10 cm through research grade noble gas in the target cell before exiting through a 1.2-mm-diam knife-edge aperture. The gas pressure inside the target cell is measured by a calibrated capacitance manometer and a signal conditioner, which also provides a feedback voltage to a solenoid valve controller to maintain the gas pressure at a preset value. The target density n is determined from the target gas pressure and temperature. The target thickness π , which is equal to the target density n multiplied by the effective scattering length l ($\pi=nl$), is varied over the range of $\pi=0$ to $\sim 3 \times 10^{14}$ atoms/cm² by changing the noble-gas pressure in the target cell. The effective scattering length is assumed to be equal to the geometri-

cal length of the target cell ($l = 3.10$ cm). A discussion of this assumption is given in Ref. [11].

After the incident beam passes through the target cell, the fast, scattered beam enters the zero-degree beam-entrance port of the charge-state analyzing magnet. The magnetic field of the magnet is adjusted to deflect the H^- and H^+ scattered ion beams I_{-1} and I_1 , respectively, into shielded Faraday cups attached to the $\pm 30^\circ$ beam-exit ports. The H^0 atoms pass undeflected through the magnet and enter the neutral detector connected to the zero-degree beam-exit port of the magnet. Electrometers are used to measure the beam currents entering the Faraday cups and the neutral detector. The I_{-1} and I_1 ion currents, the neutral detector current $S_0(\pi)$, and the noble-gas pressure p are input into a microcomputer for data analysis. The combination of incident and scattered beam currents measured as a function of various target thicknesses makes up what is referred to in this paper as a data set.

The incident H^- ion current $I_{-1}(0)$, with no noble gas in the target cell, and the background H^+ and H^0 ion currents $I_1(0)$ are measured at the beginning and end of a data set. For this experiment, the background current $I_1(0)$ is typically less than 0.1% of the value of $I_{-1}(0)$. The value of $I_{-1}(0)$ typically changes by 1–5% from the beginning to the end of a data set. At each target cell pressure, the assumed value of $I_{-1}(0)$ is obtained by linearly interpolating between the values of $I_{-1}(0)$ measured at the start and end of the data set. After a complete data set is acquired, the data acquisition program is terminated and the data file is input into a separate analysis program for determination of the resulting cross sections.

B. Data analysis

The charge-state composition of the incident H^- ion beam evolves as it passes through the noble-gas target due to charge-changing collisions with noble-gas atoms. The measured H^+ ion fraction F_1 is defined to be the background-subtracted flux of scattered protons divided by the flux of incident H^- ions:

$$F_1(\pi) \equiv \frac{I_1(\pi) - I_1(0)}{I_{-1}(0)}. \quad (1)$$

Assuming a pure incident H^- ion beam and at sufficiently low values of target thickness π , the solution to the rate equations for the H^+ ion fraction can be well represented by a quadratic function of target thickness (see, for example, Refs. [9] and [12]).

$$F_1 = \sigma_{-11}\pi + \frac{1}{2}[\sigma_{-10}\sigma_{01} - \sigma_{-11}(\sigma_{-10} + \sigma_{-11} + \sigma_{10} + \sigma_{1-1})]\pi^2 + \dots, \quad (2)$$

where σ_{ij} is the total cross section for the charge-changing process $i \rightarrow j$.

The $F_1(\pi)$ growth curves exhibit a supralinear dependence on target thickness that is represented very well by a quadratic function of π for all of the energies covered in this study. This supralinear curvature is expected from

the magnitudes of the various cross sections contributing to the quadratic component in Eq. (2). The absolute double-electron detachment cross section σ_{-11} is directly determined for each data set by fitting the H^+ ion fraction $F_1(\pi)$ to a quadratic function of π using the weighted least-squares method. The cross section will be equal to the linear coefficient of this fit, as is seen from Eq. (2). Because of the supralinear dependence of the F_1 growth curve on target thickness, a linear analysis of the growth curves will return larger DED cross-section values than the more accurate DED cross sections obtained from quadratic analyses of the growth curves.

To demonstrate the differences between the linear and quadratic analysis methods, we compare the linear fit cross sections σ_{-11}^L obtained from different target thickness ranges of the F_1 growth curve of a representative data set for a helium target gas. The resulting values of σ_{-11}^L are plotted at the upper limit of the corresponding target thickness fit range in Fig. 1. The solid line is a linear fit, weighted by the number of data points in the target thickness range corresponding to each value of σ_{-11}^L . As shown in Fig. 1, the value of σ_{-11}^L increases as the maximum target thickness used in the linear analysis fit increases. The value of σ_{-11}^L obtained from the entire target thickness range (see Fig. 1) of the data set is 12% larger than the zero target thickness intercept of the solid line. By contrast, the value of σ_{-11} obtained from a quadratic fit to the F_1 growth curve over the entire target thickness range of this data set differs only by 0.8% from the extrapolated zero-thickness intercept of σ_{-11}^L . This close agreement of σ_{-11} with the extrapolated zero target thickness value of the linear-fit cross sections is typical of

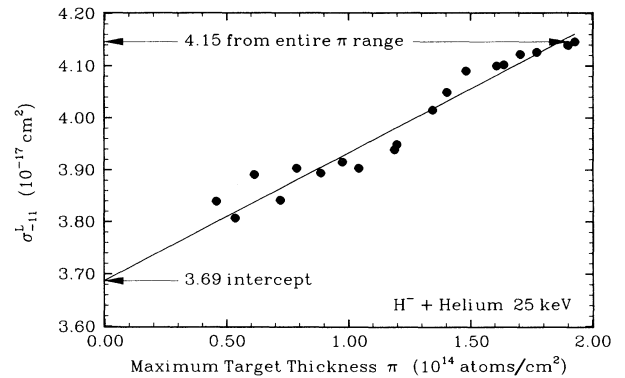


FIG. 1. The σ_{-11}^L cross sections obtained from linear fits to a typical F_1 growth curve for H^- plus helium collisions as a function of reducing the maximum helium target thickness. Solid circles, total cross-section values from a linear fit of the growth curve data from zero target thickness up to the maximum target thickness used in the fit; solid line, weighted linear fit of the cross-section values obtained from the linear fits of the growth curve data. Arrows indicate the extrapolated zero target thickness intercept from the weighted linear fit of the σ_{-11}^L values and the σ_{-11}^L value obtained from a linear fit of the entire data set. The σ_{-11} from a quadratic fit analysis of this data set gives a cross-section value of 3.72×10^{-17} cm 2 in excellent agreement with the extrapolated zero target thickness value of σ_{-11}^L .

all of the data sets for which both linear-fit and quadratic-fit analyses were made.

III. RESULTS AND DISCUSSION

A. Present experimental results

The absolute values of the total double-electron detachment cross sections, σ_{-11} , for H^- ion impact on helium, neon, and argon atoms measured in this experiment are plotted as a function of collision energy in Figs. 2(a), 2(b), and 2(c), respectively, and tabulated in Table I. The error bars associated with the present data shown in Fig.

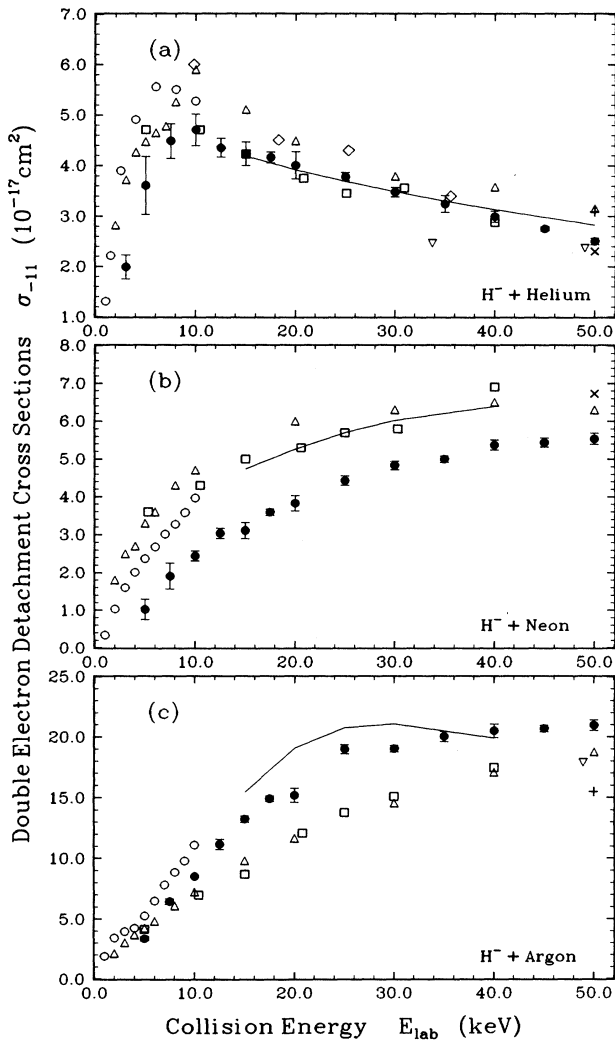


FIG. 2. Double-electron detachment cross section σ_{-11} as a function of the incident H^- ion energy for impact on (a) helium, (b) neon, and (c) argon target atoms. Solid circles, present experimental results; triangles, Williams [1]; open circles, Risley [2]; boxes, Fogel, Ankudinov, and Slabospitskii [3]; diamonds, Tsuji *et al.* [4]; +, Heinemeier, Hvelplund, and Simpson [5]; \times , Anderson *et al.* [6]; inverted triangles, Lichtenberg, Bethge, and Schmidt-Böcking [7]; solid curve, present semiempirical calculation.

2 are one weighted standard deviation. The uncertainties in the absolute values of the double-electron detachment cross sections reported in this paper depend on the uncertainties in the measurements of the noble-gas target thickness and the hydrogen ion and atom currents. These are discussed in detail in Ref. [11]. The uncertainty in the noble-gas target thickness, $\pi = nl$, is obtained by adding the individual uncertainties in quadrature, amounting to 2.7%. The uncertainties in the measurements of the ion currents depend on the accuracy of the electrometers, the collection efficiency of the detectors, and the effect of beam losses due to misalignment of the beam or scattering of the hydrogen ions through angles greater than the solid angles subtended by the detectors. The total uncertainty in the ion currents is obtained by adding the individual uncertainties associated with the ion beam measurements in quadrature. This results in a total uncertainty in the ion currents of 2.1%. The estimated total systematic uncertainty in the experimental values of σ_{-11} is assumed to be constant throughout the present energy range and is obtained by adding in quadrature the uncertainties in π (2.7%) and the ion currents (2.1%). The systematic uncertainty in the experimental values of σ_{-11} is then estimated to be 3.4%. This compares with the statistical uncertainties in σ_{-11} , which range from 1.6% to 7.7% for collisional energies > 7.5 keV. The estimated uncertainty in the collisional energy is 1%. Because the total cross sections are relatively slow-varying in collision energy, this uncertainty in the H^- ion kinetic energy will have a negligible effect on the cross-section values. The statistical uncertainties in the weighted averages of the cross sections σ_{-11} at each energy are the weighted standard deviations of the cross sections. The weighted standard deviation [13] is obtained by weighting the square deviation from the mean of each measurement of the cross section σ_{-11} by the variance in the least-squares quadratic fit to the corresponding data for the F_1 fraction.

Because all three charge-state, scattered beam components were measured in the present experiment, an alternate analysis method is available in principle as an independent verification of the DED cross sections. The leading terms of the scattered H^- ion fraction, F_{-1} , will be

$$F_{-1}(\pi) = 1 - (\sigma_{-10} + \sigma_{-11})\pi + \text{higher-order terms} . \quad (3)$$

The measured single-electron detachment cross sections σ_{-10} reported in Ref. [11] are subtracted from the linear coefficients ($\sigma_T = \sigma_{-10} + \sigma_{-11}$) of the H^- ion attenuation curves, and the DED cross sections σ_{-11} can then be obtained, as seen from Eq. (3). However, in the present measurements, the weighted standard deviations in the single-electron detachment cross sections and the H^- attenuation cross sections σ_T are typically of the same order of magnitude as the DED cross sections. Thus, one would expect only qualitative agreement between the DED cross sections obtained from the alternate method and the present DED cross sections. This is what is ob-

TABLE I. Experimental and calculated values of the total double-electron detachment cross sections σ_{-11} for H^- ions incident on helium, neon, and argon atoms. The systematic uncertainty in the experimentally determined σ_{-11} is 3.4%. The statistical uncertainties in each value of σ_{-11} are listed in the table and are one weighted standard deviation.

Laboratory collision energy (keV)	Helium		Neon		Argon	
	Experiment (10^{-17} cm 2)	Calculation	Experiment (10^{-17} cm 2)	Calculation	Experiment (10^{-17} cm 2)	Calculation
3.0	1.99±0.23					
5.0	3.61±0.57		1.02±0.27		3.35±0.19	
7.5	4.49±0.35		1.91±0.34		6.44±0.23	
10.0	4.71±0.32		2.44±0.14		8.50±0.03	
12.5	4.35±0.18		3.03±0.13		11.13±0.43	
15.0	4.23±0.23	4.18	3.11±0.21	4.74	13.24±0.24	15.4
17.5	4.16±0.11		3.59±0.07		14.92±0.22	
20.0	4.01±0.27	3.92	3.82±0.20	5.26	15.20±0.58	19.1
25.0	3.78±0.08	3.69	4.43±0.13	5.70	18.98±0.38	20.8
30.0	3.48±0.09	3.49	4.83±0.11	6.02	19.02±0.27	21.1
35.0	3.25±0.17	3.31	5.00±0.08		20.02±0.42	
40.0	3.00±0.11	3.14	5.37±0.14	6.39	20.49±0.56	19.9
45.0	2.75±0.04	2.98	5.44±0.12		20.70±0.26	
50.0	2.50±0.06	2.83	5.54±0.15		20.97±0.44	

served, with the typical percentage difference being 30% between the DED cross sections obtained from the two methods.

B. Previous experimental results

Selected measurements of the DED cross sections reported by other investigators [1–7] for H^- ions incident on helium, neon, and argon atoms are also shown in Figs. 2(a), 2(b), and 2(c), respectively. References [1] and [3–7] determined the cross sections directly from measurements of the growth of the H^+ ion current with increasing target thickness. The double-detachment cross sections reported by Williams [1] are determined from a linear analysis of his H^+ ion fraction growth curves, and the reported absolute uncertainty in the values of σ_{-11} is 8%. Williams reports values of σ_{-11} , which are about 10–40% larger than the present values for helium and neon targets, whereas for an argon target Williams's values of σ_{-11} are smaller than the present values. Consistent with the discussion concerning the supralinear dependence of the fraction F_1 , we find that the values of σ_{-11}^L obtained from a linear fit to the present growth curve data for helium and neon targets are generally in better agreement with the corresponding cross-section results of Williams in both the energy dependence and the magnitude of the DED cross sections. Anderson *et al.* [6] also performed linear analyses of their growth curves for the measurements of σ_{-11} in the 50–200-keV collision energy range. The DED cross sections at the one energy of overlap with the present results are in reasonable agreement with the present measurements of σ_{-11} at 50 keV for helium targets but are much larger than the present results for a neon target. Therefore, the discrepancies between the present results and the results of previous researchers may be at least partially attribut-

ed to the difference between the method of linear analysis and the present method of quadratic analysis of the F_1 growth curves. In the case of argon targets, we do not have an explanation at present for the fact that the present results are larger than the previously reported DED cross sections shown in Fig. 2(c) above collision energies of 10 keV.

Several groups accounted for the curvature in the low target thickness region of their growth curves. The DED cross sections reported by Fogel, Ankudinov, and Slabospitskii [3] were obtained by fitting the ratio of the H^+ ion current and the H^- ion current to a quadratic function of the target thickness, so one should expect good agreement with the present results. The DED cross sections are in the best agreement with the present results in both the magnitudes and the energy dependence of the DED cross sections for helium targets, but they agree only in the energy dependence of the DED cross sections for neon and argon targets. Again, we cannot offer an explanation for the disagreement between the two sets of measurements for neon and argon targets. Lichtenberg, Bethge, and Schmidt-Böcking [7] measured the double-electron detachment cross sections at impact energies ≥ 34 keV for a variety of target species, including helium and argon. While the present value of σ_{-11} at an energy of 50 keV for helium targets is in good agreement (2% difference) with the value of σ_{-11} at 50 keV reported by Lichtenberg, Bethge, and Schmidt-Böcking [7], the DED cross sections of Ref. [7] display a different energy dependence than the results of Anderson *et al.* [6] at high energies and of the present measurements from 35 to 50 keV. For helium targets at 34 keV, the value of σ_{-11} reported by Lichtenberg, Bethge, and Schmidt-Böcking in Ref. [7] is about 30% lower than the present value of σ_{-11} at 35 keV; and at energies above 50 keV, the data of Ref. [7] show the DED cross sections increasing with increasing

energy until a local maximum in the cross section is reached at about 88 keV. This is in contrast with the other measurements, which show the DED cross sections decreasing with increasing collision energy in this collisional energy region. For argon targets, the Lichtenberg, Bethge, and Schmidt-Böcking results at 50 keV are lower than the present results by 15%.

C. Theoretical calculations

We have not found any previous *ab initio* calculations in the literature of double-electron detachment in intermediate-energy collisions of H^- ions incident on helium, neon, and argon. However, at high-impact energies, double-electron detachment cross sections for H^- ions incident on helium atoms (and various other gases) have been calculated by Riesselmann *et al.* [14] using the free-collision model (FCM) and a geometric model similar to the geometric models used by Bates and Walker [15] and Dewangan and Walters [16] to calculate single-detachment cross sections. In the calculation of Ref. [14], the strongly and weakly bound electrons of the H^- ion are assumed to scatter independently in the collision with the target atom; the electron-loss cross sections corresponding to direct scattering of each electron are separately obtained from semiempirical FCM calculations; and these cross sections are combined, using a geometric model, to obtain the single- and double-electron-loss cross sections for H^- plus He collisions. Their results, which cover the 90 keV to 1.4 GeV energy range, are in good agreement with the experimental data.

In this section, we describe a calculation of the double-electron detachment cross sections for H^- plus He collisions in the 15 to 50-keV energy range that is based on the geometric model of Riesselmann *et al.* [14]. This model uses the experimental values of the single-electron detachment cross section σ_{-10} for H^- ions and the electron-loss cross section σ_{01} for H^0 atoms incident on the noble-gas target atoms. As the collision energy decreases, the electron-electron correlation effects are expected to become increasingly important; therefore, we do not extend this model lower than 15 keV. Following the approach of Riesselmann *et al.* [14], the cross section Q_i for the loss of electron i of the H^- ion due to direct scattering by a target atom is represented by a disk with an area equal to the value of Q_i , where $i=1$ corresponds to the strongly bound projectile electron and $i=2$ corresponds to the weakly bound projectile electron. As viewed by the target, the centers of the disks corresponding to the cross sections Q_1 and Q_2 are separated by a distance d , where the disks may overlap. (See Fig. 3 of Ref. [14] for a graphical depiction of these parameters.) For a given vector separation \mathbf{R} of the projectile electrons, the distance $d=R\sin\theta$, where R is the magnitude of the vector \mathbf{R} and θ is the angle between the direction of incidence and the vector \mathbf{R} . Riesselmann *et al.* [14] have shown that the average area of overlap, $\langle A \rangle$, of the two disks can be interpreted as the double-electron-loss cross section due to direct scattering of both projectile electrons on the target atom, and the area $Q_1+Q_2-2\langle A \rangle$ can be interpreted as the single-

electron-loss cross section due to direct scattering. In the calculation described below, the double-electron detachment cross sections are determined from the experimental values of σ_{-10} and σ_{01} by constraining the quantity $Q_1+Q_2-2\langle A \rangle$ to agree with the experimental values of the single-electron detachment cross section σ_{-10} , using an iterative procedure.

We assume that the value of the electron-loss cross section Q_1 of the strongly bound electron of the H^- ion at a given projectile velocity is equal to the known experimental value [17,18] of the electron-loss cross section σ_{01} at the same velocity. In step 1 of the iterative procedure, the starting value of the electron-loss cross section of the weakly bound projectile electron Q_2 at a given projectile velocity is taken to be equal to the present experimental value of σ_{-10} at the same velocity. Using this value of Q_2 , we calculate the average area of overlap $\langle A \rangle$ of the circles corresponding to the electron-loss cross sections Q_1 and Q_2 . The area of overlap, $A(l_1, l_2, d)$, of the two circles is determined by the distance $d=R\sin\theta$; the radii of the two circles, l_1 and l_2 , where $l_i=(Q_i/\pi)^{1/2}$; and Eq. (10b) of Ref. [14]. The value of $\langle A \rangle$ is obtained by averaging the area of overlap $A(l_1, l_2, d)$ over all magnitudes and orientations of the vector \mathbf{R} , using Eq. (10a) of Ref. [14] and the expression for the normalized distribution function $P(R)$ for the separation R between the electrons of the H^- ion in Ref. [14]. In step 2, a new value of Q_2 is calculated by setting the experimental value of σ_{-10} equal to the quantity $Q_1+Q_2-2\langle A \rangle$ and solving for the cross section Q_2 in terms of the quantities σ_{-10} , Q_1 , and $\langle A \rangle$. In step 3, a new value of the average area of overlap $\langle A \rangle$ is calculated from the value of Q_2 obtained in step 2. Steps 2 and 3 are then repeated until the calculated value of $\langle A \rangle$ converges satisfactorily. In the present calculation, the value of $\langle A \rangle$ converges in a few iterations.

We note that in the 5 to 50-keV range of collision energies, the experimental values of the cross section σ_{01} reported by different investigators [8] differ by as much as 30%. However, only Williams [17] and Fogel *et al.* [18] have obtained the values of σ_{01} directly from the growth of the H^+ ion collision products. Therefore, we choose to use the values of σ_{01} reported by Refs. [17] and [18], which generally agree to within 10% in the 15 to 50-keV energy range for helium targets. The values of σ_{01} used in the present calculation are obtained by fitting the data of Refs. [17] and/or [18] to a polynomial of the collision energy in the 15 to 50-keV energy region. The values of σ_{-10} used in the present calculation are obtained by fitting the single-electron detachment cross sections σ_{-10} given in Ref. [11] to a quadratic function of the logarithm of the collision energy in the 15 to 50-keV energy region. The present calculation is sensitive to the input experimental values of σ_{01} and σ_{-10} . For example, calculations of σ_{-11} carried out by using input values of σ_{01} that differ by 30% produce calculated values of σ_{-11} that differ by about that same amount.

Following Riesselmann *et al.* [14], we include the contribution of "electron shake-off," in which one projectile electron of H^- is detached due to direct scattering and

the other projectile electron is excited to a continuum state of the H^0 atom, resulting in the loss of both electrons from the H^- projectile ion. The double-electron detachment cross section is obtained from the value of Q_1 , the final values of Q_2 and $\langle A \rangle$ as determined by the iteration procedure described above, and the equation $\sigma_{-11} = (1 - P_1 - P_2)\langle A \rangle + P_2 Q_1 + P_1 Q_2$. In this equation, $P_1 = 6.55 \times 10^{-4}$ and $P_2 = 9.63 \times 10^{-3}$ are the probabilities that the strongly bound and weakly bound electrons, respectively, are "shaken off" in the collision [14]. In the present calculation, the contribution of electron shake-off to the DED cross section for helium targets is less than 5% of the calculated value of σ_{-11} over the 15 to 50-keV energy region.

As shown in Figs. 2(a)–2(c), the calculated values of σ_{-11} are generally in good agreement with the present experimentally determined values of σ_{-11} for helium targets, are in fair agreement for argon targets, and overestimate the present measured DED cross sections for neon targets. We have also calculated the values of σ_{-11} for collision energies from 100 to 200 keV for helium targets using the experimental values of σ_{-10} and σ_{01} reported by Anderson *et al.* [6]. We find that the calculated values of σ_{-11} are in good agreement with the corresponding experimental data of Ref. [6] and the semiempirical calculation of Riesselmann *et al.* [14]. At collision energies below 25 keV, the projectile velocity is comparable to or less than the velocity of the strongly bound electron relative to the center of mass of the H^- ion, and electron correlation may play an important role in double-electron detachment collisions at these energies. Because the electron shake-off contribution (in this calculation) is of the same order of magnitude as the uncertainties in the present DED cross-section measurements, measurements of target state-resolved DED total cross sections and/or DED angular differential cross sections, coupled with an *ab initio* theoretical model, will be needed to clarify the actual role electron correlation plays in this charge-changing process.

IV. SUMMARY

The absolute values of the total cross sections for double-electron detachment in collisions between 5- to

50-keV H^- ions and helium, neon, and argon atoms have been measured by simultaneously measuring the growth of the H^+ ion and the attenuation of the H^- ion scattered beam components. The H^+ ion growth curve fractions have a slightly nonlinear dependence on the target thickness, which is well described by a quadratic function of the target thickness over the range of target thicknesses used in the present experiments. The present double-electron detachment (DED) cross sections σ_{-11} for helium targets are in the best agreement with the previously reported measurements compared to the cases of the other two noble-gas (neon and argon) target species. At this time we cannot offer a systematic explanation for this disagreement. Further studies of double-electron detachment for neon and argon targets are warranted in light of these discrepancies. Target-state-resolved measurements of DED for all three target species would reveal the extent that the DED process is accompanied by target excitation and may provide information on the mechanisms leading to electron detachment in these collisional systems.

The calculations of DED based on a semiempirical theory are in general agreement with the present experimental data for helium targets, but the calculation overestimates the DED cross sections for neon and argon targets. *Ab initio* theoretical models of the double-electron detachment cross sections are still needed and, coupled with the state-resolved measurements referred to above, should provide a better physical insight into electron detachment for these fundamental negative-ion-atom collision systems.

ACKNOWLEDGMENTS

The authors are appreciative of useful discussions with D. G. Seely, M. Kimura, and L. W. Anderson. This work is supported by a grant from the Division of Chemical Sciences, Office of Basic Energy Sciences, Office of Energy Research, U.S. Department of Energy.

-
- [1] J. F. Williams, *Phys. Rev.* **154**, 9 (1967).
 - [2] J. S. Risely, *IEEE Trans. Nucl. Sci.* **NS-26**, 1027 (1979).
 - [3] Ia. M. Fogel, V. A. Ankudinov, and R. E. Slabospitskii, *Zh. Eksp. Teor. Fiz.* **32**, 453 (1957) [*Sov. Phys. JETP* **5**, 382 (1957)].
 - [4] H. Tsuji, J. Ishikawa, T. Maekawa, and T. Takagi, *Nucl. Instrum. Methods B* **37/38**, 231 (1989).
 - [5] J. Heinemeier, P. Hvelplund, and F. R. Simpson, *J. Phys. B* **9**, 2669 (1976).
 - [6] C. J. Anderson, R. J. Girnius, A. M. Howald, and L. W. Anderson, *Phys. Rev. A* **22**, 822 (1980).
 - [7] W. J. Lichtenberg, K. Bethge, and H. Schmidt-Böcking, *J. Phys. B* **13**, 343 (1980).
 - [8] H. Tawara and A. Russek, *Rev. Mod. Phys.* **45**, 178 (1973).
 - [9] E. W. McDaniel, J. B. A. Mitchell, and M. E. Rudd, *Atomic Collisions—Heavy Particle Projectiles* (Wiley, New York, 1993).
 - [10] J. S. Allen, X. D. Fang, and T. J. Kvale, *Nucl. Instrum. Methods B* **79**, 106 (1993).
 - [11] T. J. Kvale, J. S. Allen, X. D. Fang, A. Sen, and R. Matulioniene, *Phys. Rev. A* **51**, 1351 (1995).
 - [12] T. J. Kvale, J. S. Allen, A. Sen, X. D. Fang, and R. Matulioniene, *Phys. Rev. A* **51**, 1360 (1995).
 - [13] P. R. Bevington, *Data Reduction and Error Analysis for the Physical Sciences* (McGraw-Hill, New York, 1969).
 - [14] K. Riesselmann, L. W. Anderson, L. Durand, and C. J. Anderson, *Phys. Rev. A* **43**, 5934 (1991); **46**, 7329 (1992). In the present calculation, we used the correct form of the function $P(R)$ given in *Phys. Rev. A* **46**, 7329 (1992).

- [15] D. R. Bates and J. C. Walker, Proc. Phys. Soc. London **90**, 333 (1967).
- [16] D. P. Dewangan and H. R. J. Walters, J. Phys. B **11**, 3983 (1978).
- [17] J. F. Williams, Phys. Rev. **153**, 116 (1967).
- [18] Ia. M. Fogel, V. A. Ankudinov, D. V. Pilipenko, and N. V. Topolia, Zh. Eksp. Teor. Fiz. **34**, 579 (1958) [Sov. Phys. JETP **34**, 400 (1958)].